Wang et al., Afr J Tradit Complement Altern Med. (2016) 13(6):121-129
10.21010/ajtcam. v13i6.17

STUDIES ON THE INTERACTION BETWEEN TRIPTOLIDE AND BOVINE SERUM ALBUMIN (BSA) BY SPECTROSCOPIC AND MOLECULAR MODELING METHODS

Haidong Wang[1], Hailang Shi[2], Jie Pang[1], Xingfa Song[1], Caiyun Xu[1], Zengxian Sun[1]*

[1]Department of Pharmacy, The First People's Hospital of Lianyungang, Jiangsu, Lianyungang 222002, PR China.[2]Department of Pharmacy, Yanqi Hospital of Xinjiang Agriculture second Division Xinjiang,Yanqi 841100, PR China.

*** Corresponding author E-mail**: 410769467@qq.com

Abstract

Background: Triptolide is a major active constituent isolated from Tripterygiumwilfordii Hook F, a Chinese herbal medicine. This study investigated the intermolecular interaction between triptolide and bovine serum albumin (BSA).
Materials and Methods: The fluorescence, circular dichroism (CD) and molecular docking methods were used to investigate the intermolecular interaction between triptolide and BSA. The binding constant, the number of binding sites, binding subdomain and the thermodynamic parameters were measured.
Results: The results of this experiment revealed that the intrinsic fluorescence of BSA was effectively quenched by triptolide via static quenching. The experimental results of synchronous fluorescence and CD spectra showed that the conformation of BSA was changed in the presence of triptolide.
Conclusion: It indicated that triptolide could spontaneously bind on site II (subdomain IIIA) of BSA mainly via hydrogen bonding interactions and Van der Waals force.

Key words : fluorescence quenching ; triptolide ; bovine serum albumin ; molecular docking methods ; synchronous fluorescence

Introduction

The Chinese herbal medicine Tripterygiumwilfordii Hook F, also called Lei gong teng in a Chinese, is used for the treatment of various illnesses for centuries in China (Cameron et al., 2009). Triptolide (Figure 1), a major active diterpenetriepoxide constituent isolated from T. wilfordii, has shown promising immunosuppressive (Liu et al., 2005), anticancer (Yang et al., 2003; Panichakul et al., 2002; Lou et al., 2005), antifertility (Matlin et al., 1993) activities.

It is generally known that triptolide has a narrow therapeutic window and could caused severe toxicity, such as significant hepatotoxicity and reproductive toxicity (Liu et al., 2010; Ni et al., 2008; Mei et al., 2005), which limits its application.

Serum albumin, which is the most soluble and plentiful protein present in cardiovascular system, accounts for 50% to 65% of the plasma levels of total protein (Carter and Ho, 1994).

It has an extensive ligand binding capacity and has many biological functions in deporting and transporting several of exogenous and endogenous compounds, for instance metal ions, fatty acids, and drugs in the bloodstream (Tian et al., 2003; Wang et al., 2006). Most drugs and biological active small molecules bind with serum-albumin strongly and reversibly, forming a drug–protein complex (Diao et al., 2013); the drug–protein interaction affects the distribution, metabolism, efficacy, toxicity and stability during the therapeutic process (Diao et al., 2015).

Numerous studies have focused on the interaction between small molecule drugs and serum-albumin, which will offer further insight into the mechanism and metabolic processes of target drugs.

Bovine serum albumin (BSA) is one of the most completely researched serum albumin proteins in experiments, on account of its low cost, availablility upon request, uncommon ligand-binding properties and 76% sequence identity with human serum albumin (HSA). (Mallick, et al., 2005; Wang et al., 2008; MacManus-Spencer et al., 2010).

The present study aimed at investigating the interaction between triptolide and BSA using fluorescence spectrum, circular dichroism (CD), and molecular docking. This study also determined the quenching mechanisms, association constants, thermodynamic parameters, binding site number, binding force and location, and conformation in the interaction. The results of this study provide valuable information on the mechanisms underlying triptolide action and pharmacokinetics in vivo.

Experimental

Reagents

The reference standard of triptolide (98% purity) was provided by PI&PI Technologies, Inc. (Guangdong, China). Tris buffer was gained through Sinopharm Chemical Reagent Co., Ltd (Pudong, China; purity ≥ 99.5%). BSA was purchased from Sigma-Aldrich Chemicals (St. Louis, MO, USA) and its solution ($1.5\times10-5$ mol•L^{-1}) was prepared in buffer solution of pH 7.4 Tris–HCl (0.1 mol•L^{-1} NaCl was added to maintain ionic strength). Phenylbutazone and ibuprofen were supplied by National Institutes for the Control of Pharmaceutical and Biological Products (Beijing, China) and were dissolved in about 1.0 mL methanol and diluted with Tris–HCl buffer solution to make a 1.5×10^{-5} mol•L^{-1} stock-solution, then for ascertaining the binding sites of triptolide at BSA. All other chemicals used were of highest purity available and the ultrapure water (resistivity > 18.2 MΩ) was generated by a Milli-Q apparatus (Millipore, Molsheim, France). All of the reagents and solvents were stored at 4oC and diluted as required.

Apparatus and measurements

Fluorescence Measurements

The BSA solution containing 1.5×10^{-5} mol•L^{-1} was diluted by serial additions of triptolide stock-solution. The triptolide concentrations were ranged from zero to 10.0×10^{-6} mol•L^{-1}.

All fluorescence spectra were obtained from a PerkinElmer LS-55 spectrofluorometer (Shelton, USA) assembled with a 1 cm quartz cell using 289 nm as the excitation wavelength, and the emission spectra were logged within the range of 305 nm to 500 nm at three differing temperatures (298, 302 and 310 K). The emission slit and excitation slit widths were both 7 nm, and the photomultiplier voltage was set at 750 V. The scanning speed was fixed at 500 nm/min. In the binding marker competition experiments, fluorescence spectra were carried out at 298 K with a wavelength of 289 nm for excitation in range of 305 nm to 500 nm. The molar concentration ratio of BSA to phenylbutazone/ibuprofen was 1:1, and then triptolide was gradually injected into the BSA–phenylbutazone and BSA–ibuprofen systems.

UV–vis absorption measurements

The absorption spectrums were processed on S600 UV spectrophotometer (Analytikjena, German) outfitted with 1.0 cm quartz windows. The wave length ranged from 305 nm to 500 nm.

Circular dichroism (CD) measurements

The CD spectrum of BSA in the existence of triptolide was registered between 200 and 230 nm at 298 K and under the constant nitrogen flush with a Jasco J-810 Spectropolarimeter (Jasco, Tokyo, Japan). The molar concentration ratio of triptolide to BSA was changed from 0:1 to 1:1 and 4:1. Each CD spectrum was gained via a 1 mm cell at a bandwidth of 1 nm and a scanning speed of 200 nm/min.

Synchronous fluorescence spectroscopy

The synchronous fluorescence spectrums were recorded by sweeping the solutions of BSA containing a serial concentration of triptolide fixing $\Delta\lambda$ at 60 nm and 15 nm. The emission and excitation slit widths, scan speed and photomultiplier voltage were similar to those in the fluorescence measurements

Molecular docking

The 3D structure of triptolide was generated and optimized using Chemoffice Ultra software (Version 10.0, CambridgeSoft.com, USA) and Gaussian 03 software (Gaussian Inc., Wallingford, USA). UniProtKB: P02769, the crystalline structure of BSA, was acquired from the SWISS-MODEL Repositor (http://swissmodel.expasy.org/repository/?pid = smr01&zid = async) and was analyzed with NAMD 2.9 software and CHARMM27 force field parameters. The bumps were fixed, all side-chains were repaired, and the polar H atoms were added.

Docking calculations were performed by AutoDock 4.0. Kollman united atom type charges and Essential polar hydrogen atoms were added as well as waters were removed from protein PDB files using the AutoDock software tools. The ligand roots of triptolide were probed and the rotatable bonds were determined. It formed the Grid maps of 60Å×60Å×60Å grid points and 0.375 Å spacing. These centers of grid boxes were located in points (9.630, –23.483, –7.475), points (–2.515, –7.086, 5.282) and points (16.897, 8.738, –16.208). After the complete generation of the grid map, docking simulations were run by Lamarckian genetic algorithm (LGA) and the two pt GA crossover mode for 100 times. The following autodock parameters will be used: population size: 150, and maximum numbers of energy evaluations: 2,500,000, with numbers of generations: 27000.

Results and Discussion

Fluorescence quenching of BSA in the existence of triptolide

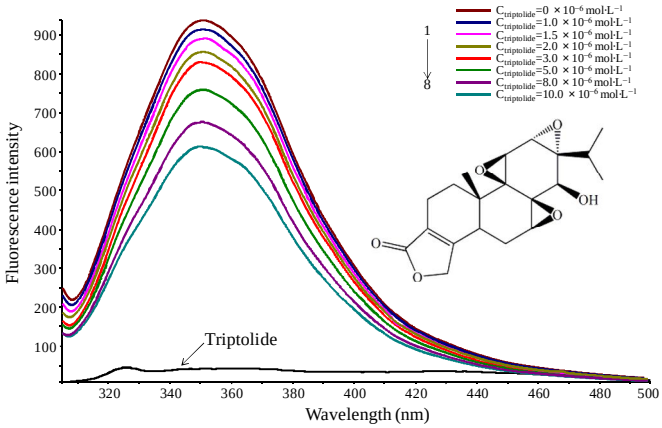

Figure 1: Chemical structure of triptolide and the fluorescence quenching spectra of BSA at different concentrations of triptolide (T=298 K, pH=7.4); from curve 1 to 8, C_{BSA}= 5.0×10^{-6} mol·L^{-1}, $C_{triptolide}$=0, 1.0, 1.5, 2.0, 3.0, 5.0, 8.0, 10.0×10^{-6} mol·L^{-1}

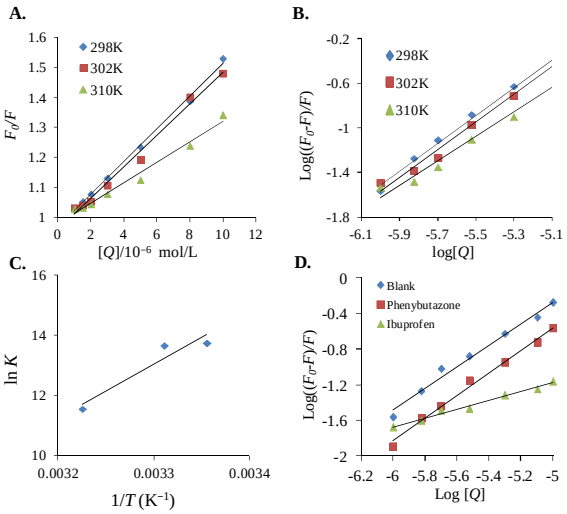

Figure 2*: A. Stern-Volmer plot for the quenching of BSA by triptolide at different temperatures [a]. **B.** Double-log plots of triptolide quenching effect on BSA fluorescence at different temperatures [a]. Double-log plots of triptolide quenching effect on BSA fluorescence in at 298 K in the presence of site markers. **C**. The Van't Hoff plot for the interaction of BSA and triptolide at different temperatures. D. Double-log plots of triptolide quenching effect on BSA fluorescence in at 298 K in the presence of site markers [a,b].

[a] $C_{BSA}=5.0\times10^{-6}$ mol·L^{-1}, $C_{triptolide}$ =1.0, 1.5, 2.0, 3.0, 5.0, 8.0, 10.0×10^{-6} mol·L^{-1}

[b] $C_{BSA}=C_{phenylbutazone}= C_{ibuprofen}=5.0\times10^{-6}$ mol·L^{-1}

* F and F_0 are the fluorescence intensities in the presence and absence of quencher

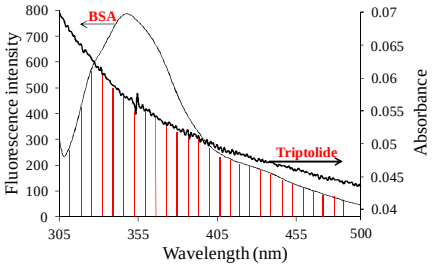

Figure 3: Overlap of fluorescence emission spectrum of BSA and UV absorption spectrum of triptolide ($C_{BSA}=C_{triptolide}=2\times10^{-6}$mol·L^{-1}) at 298 K.

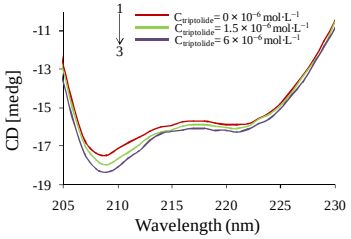

Figure 4: CD spectra of free bovine serum albumin (BSA) (1) and triptolide–BSA complex (2,3): The concentration of BSA was 1.5×10^{-6} mol·L^{-1}. The concentrations of triptolide from 1 to 3 were 0.00, 1.5×10^{-6}, 6×10^{-6} mol·L^{-1}, respectively. CD, circular dichroism.

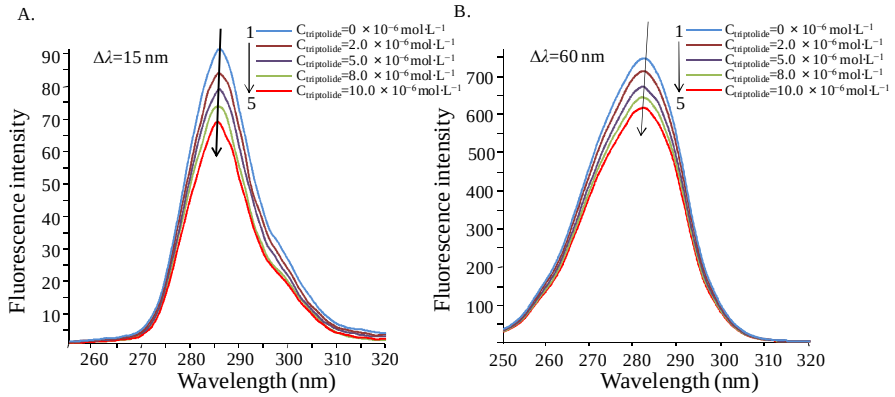

Figure 5: Synchronous fluorescence spectra of interaction between BSA and triptolide at 298 K. C_{BSA}=1.5×10^{-6} mol·L^{-1}, The concentration of triptolide from 1 to 5: 0, 1, 2, 5, 8, 10×10^{-6} mol·L^{-1} (A) Δλ=15 nm, (B) Δλ=60 nm

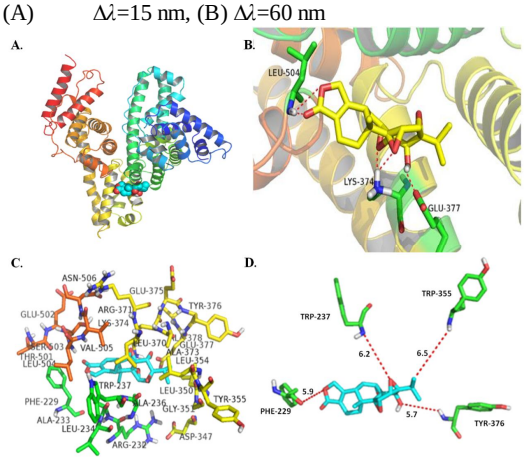

Figure 6: (A) Minimum energy docking conformation of Triptolide-BSA complex obtained from molecular docking. BSA and triptolide are presented by the cartoon structure and dots model, respectively. (B) The hydrogen bonding interaction between triptolide and amino acid residues of BSA, which are shown in complex and alone, respectively. (C) The amino acid residues surrounding triptolide within 8 Å. Triptolide is represented using azure. (D) The minimum distances between triptolide and some fluorophores residues in BSA.

Table 1: Stern-Volmer quenching constant of BSA by triptolide at different temperatures

T/K	K_{SV} (10^4·mol^{-1}·L)	K_q (10^{13} s^{-1}·mol^{-1}·L)	r
298	5.46	5.46	0.9985
302	5.26	5.26	0.9951
310	3.43	3.43	0.9913

Table 2: The binding constant and thermodynamic parameters for triptolide binding to BSA at different temperatures

T/K	*K* (10^5L·mol^{-1})	*N*	r[a]	ΔH^0 (KJ·mol^{-1})	ΔS^0 (J·mol^{-1})	ΔG_1^0 (KJ·mol^{-1})		ΔG_2^0 (KJ·mol^{-1})	r[b]
298	9.39	1.2473	0.9976	−148.6	−382	−34.07	−34.77		0.9528
302	8.62	1.2507	0.9943	−148.6	−382	−34.32	−33.24		
310	1.05	1.1085	0.9904	−148.6	−382	−29.79	−30.18		

[a]r was the correlation coefficient for the *K* values
[b]r was the correlation coefficient for the van't Hoff plot
ΔG_1^0 was evaluated from Eqs.5
ΔG_2^0 was evaluated from Eqs.6

Table 3: Binding constants of competitive experiments at 298 K

Site market	K (10^5 L·mol^{-1})	r
Blank	5.97	0.9921
Phenylbutazone	6.17	0.9958
Ibuprofen	0.00202	0.9921

Fluorescence is broadly employed to study the interaction between proteins and various drugs, has been used to provide much evidence about the quenching mechanism, binding sites and constants. BSA can generate inherent fluorescence emission band at 338 nm as the exciting at 289 nm for the existence of Trp–159 and Trp–237 residues, which show intrinsic fluorescence (Shi et al., 2014).

In this research work, our team recorded the fluorescence quenching spectra of BSA with different concentrations of triptolide by fixing an excitation wavelength of 289 nm in eight concentrations of triptolide at serial different temperatures (298, 302 and 310 K). The fluorescence curve for triptolide and BSA fluorescence intensity affected by triptolide at 298 K, were shown in Figure 1. It showed emission for triptolide at the excitation wavelength of 289 nm was so weak that should neglect the inner-filter effect of triptolide and the fluorescence intensity of BSA gradually decreased with the addition of triptolide. The phenomenon indicated the BSA intrinsic fluorescence can be quenched by triptolide.

It can classify fluorescence quenching as static quenching or dynamic quenching by mechanisms. The forming of a fluorophore–quencher complex can result in static quenching result, whereas collisional encounters will cause dynamic quenching. Static and dynamic quenching can be characterized by reliance on lifetime of the excited state and temperature. Also, dynamic quenching relies on the effect of diffusion. Lower temperatures will bright about littler diffusion coefficients. Thus, complex quenching constants can be supposed to decrease with decreasing temperature. However, the stability of complexes and static quenching constant value are likely to be decreased by high temperatures (Zhang et al., 2009). The well–known Stern–Volmer equation was utilized to calculate the quenching constant (K_{SV}) of BSA (Lakowicz, 2009).

$$F_0 / F = 1 + K_q \tau_0 [Q] = 1 + K_{SV} [Q] \quad (1)$$

$$K_q = K_{SV} / \tau_0 \quad (2)$$

where F_0 and F are the fluorescence intensities in the absence and presence of quencher, respectively; K_{SV}, τ_0 (10^{-8} s^{-1}) (Lakowicz *and* Weber,1973), k_q and [Q] represent the Stern–Volmer quenching constant, the average lifetime of the protein without the quencher, the quenching rate constant of the biomolecule and the concentration of the quencher (triptolide), respectively.

The Stern–Volmer equation was employed to calculate the Stern–Volmer quenching constant (K_{SV}) at several temperatures of 298, 302 and 310 K (Figure 2A) and the data were summarized in Table 1. The result demonstrated the Stern–Volmer quenching constant K_{SV} and temperature were negatively correlated with each other and the K_q values were far outweigh the supreme scatte collision quenching constant of the biomolecule (2×10^{10} s^{-1}·mol^{-1}·L) (Ware,1962), which indicated the triptolide emplyed a static quenching process to result the fluorescence quenching of BSA.

The binding constant (K) between the quencher and BSA and the number of binding sites (n) could be calculated using double–logarithm algorithm curve (Eq. 3) for static quenching process (Wang et al., 2006).

$$\log \frac{F_0 - F}{F} = \log K + n \log [Q] \quad (3)$$

The slope of log((F_0 –F)/F) against log[Q] curves (Double-log plots) is shown in Fig 2B and Table 2 list the corresponding values of K at three temperatures. The result indicated that K decreased as the temperature increased and n approached 1. These results were consistent with previous discussions on K_{SV}. During the interaction, only one binding site was present in BSA for triptolide.

In general, hydrogen bond, Van der Waals force, electrostatic force, hydrophobic interaction forces are the four types of non-covalent interaction between proteins and ligand. The van't Hoff plots can be used to calculate the thermodynamic parameters for elucidating the interaction between ligand and BSA. Thermodynamic laws (Ross and Subramanian) (Ross et al., 1981) determine the types of binding among different interactions, in which enthalpy change (ΔH^0), free energy change (ΔG^0) and entropy change (ΔS^0) are considered important thermodynamic parameters. On the one hand, the conditions in which $\Delta S^0<0$ and $\Delta H^0<0$, suggest that van der Waals and hydrogen bond interactions serve significant functions during the progress of binding reaction. On the other hand, the conditions in which $\Delta S^0>0$ and $\Delta H^0>0$ reflect a dominant hydrophobic interaction. $\Delta H^0<0$ and $\Delta S^0>0$ show the main force is an electrostatic effect.

Provided that the temperature would not change, these values of ΔH could be looked as a constant. Equations 4, 5, and 6 provide approximate values of ΔH^0, ΔS^0, and ΔG^0 as shown below:

$$\ln K = -\Delta H^0 / RT + \Delta S^0 / R \quad (4)$$

$$\Delta G^{0} = -RT \ln K \quad (5)$$

$$\Delta G^{0} = \Delta H^{0} - T\Delta S^{0} \quad (6)$$

Where R is the gas constant; K represents binding constant at the relevant temperature; and that T stands for experimental temperature. Figure 2C showed the plot of lnK against $1/T$. Table 2 contained these values of ΔH^{0}, ΔS^{0}, and ΔG^{0}. The negative ΔS^{0} and ΔH^{0} demonstrated Van der Waals force and hydrogen bond formation had governing functions during the binding of triptolide with BSA, whereas the negative ΔG^{0} meant that triptolide can spontaneously bind with BSA.

Binding distance between the Triptolide and the amino acid residues of BSA

Fluorescence resonance energy transfer (FRET) has been widely applied in energy conversion. Förster resonance energy transfer could be used for expressing energy transfer between the acceptor and an initially excited donor chromophore through nonradiative dipole-dipole coupling. On the basis of Förster's nonradiation energy transfer theory, E, the energy transfer efficiency, can be affected by the distance between the acceptor and donor, as well as by the transfer distance of critical energy, which can be counted using the follow-up equation (Sklar et al., 1977):

$$E = 1 - \frac{F}{F_0} = \frac{R_0^6}{R_0^6 + r^6} \quad (7)$$

where r means the distance between the acceptor and the donor. R_0 is the Förster distance of the pair of acceptor and donor while the efficiency fix at 50%. The value of R_0 can be counted with the following equation:

$$R_0^{\ 6} = 8.8 \times 10^{-25} K^2 n^{-4} \varphi J \quad (8)$$

K^2 represents the spatial orientation factor of the dipole, n represents the refractive index of medium in the wavelength range, φ is the fluorescence quantum yield of the donor, and J is the overlap integral of the absorption spectrum of the acceptor and the emission spectrum of the donor. Under these experimental conditions, K^2= 2/3, N= 1.336, φ=0.118 (Olson *and* Christ, 1996), and J were given using the equation:

$$J = \sum F(\lambda)\varepsilon(\lambda)\lambda^4 \Delta\lambda / (\sum F(\lambda)\Delta\lambda) \quad (9)$$

Where $\varepsilon(\lambda)$ and $F(\lambda)$ represent the molar absorption coefficient of the acceptor and the fluorescence intensity of the donor at wavelength λ, respectively.

Figure 3 gave the result of the overlap of the absorption spectra of triptolide and the fluorescence emission spectra of BSA at 298 K. Consequently, we obtained J = 3.55×10^{-15}cm^3·L·mol^{-1}, R_0 = 1.96 nm, r = 2.32 nm for the distance between Trp of BSA with triptolide. The binding distance r = 2.32 nm, which was less than 7 nm and follow the ruler of 0.5 R_0<r<1.5 R_0, which implied non-radiation energy transfer between BSA and triptolide occurred (Veatch and Stryer, 1997). And the value of r was greater than that of R_0, which implied the interaction process between BSA and triptolide was the static quenching.

The change of the secondary structure of BSA with Triptolide
Circular dichroism (CD) measurements

CD spectroscopy is an effective tool in monitoring the modifications about protein secondary structure on interaction with small molecules. In the ultraviolet region at 209 and 222 nm, there exhibit two negative bonds CD spectra of BSA, which are specific of α--helix secondary structure of proteins. Figure 4 showed the CD spectroscopy of BSA with triptolide within the range of 205 nm to 230 nm, which showed two characteristic minima at approximately 209 and 222 nm. This result is consistent with a previous report (Lu et al., 2007). The addition of triptolide increased the band intensity at whole wavelengths of the CD spectra after comparing curves 2 and 3 with curve 1. This result illustrated the interaction process between triptolide and BSA altered the conformation of BSA.
Mean residue ellipticity (MRE) was employed to express the α-helical content for BSA according to the following equation:

$$\text{MRE} = \frac{\text{observedCD（mdeg）}}{C_p n l \times 10} \quad (10)$$

where C_P represents molar concentration of the protein; l represents the path length; and n represents the number of amino acid residues (582 for BSA). The combined and free BSA α-helix contents could be reckoned using the following equation (Greenfield and Fasman, 1969):

$$\alpha\text{-helix} = \frac{-\text{MRE}_{209} - 4000}{33000 - 4000} \times 100\% \quad (11)$$

where MRE_{209} is an obtained value of MRE at 209 nm; 4000 is the MRE value of the random coil conformation cross and α-form at 209 nm; and 33000 means that the MRE is a pure α-helix at 209 nm.

The analysis results of the α-helix content were obtained from Equation 10 and 11. The data exhibited that the α-helix contents were added from 55.2% to 57.1% and 58.7% at molar ratios of triptolide to BSA of 1:1 and 4:1, respectively. They also indicated the addition of α-helix upon the interaction between BSA and triptolide, suggesting that triptolide associated with the amino acid residues of the backbone in BSA and stabilized BSA internal hydrogen bonding. Whether in the absence or presence of triptolide,

these shapes of the CD spectra of BSA were similar, demonstrating typical structure of BSA was also dramatically α-helix after the mix of triptolide (Hu et al., 2005). The above analyses demonstrated the conformation of BSA changed after triptolide was added.

Synchronous fluorescence spectroscopy

Synchronous fluorescence spectra can offer valuable information for microenvironment within the vicinity of the chromophore molecule (Wang et al., 2010). The emission of tryptophan (Trp) and tyrosine (Tyr) residues in molecules manifests that intrinsic fluorescence. The synchronous fluorescence shows typical information about Trp or Tyr residues when the wavelength interval (Δ□) between the emission and excitation wavelengths is fixed at 15 or 60 nm (Klajnert and Bryszewska, 2002). Figure 5 shows the change in synchronous fluorescence spectra in BSA conformation when the triptolide is added.

When triptolide concentration gradually increased, the synchronous fluorescence intensity reduced as well as the maximum wavelength of the emission peaks of Trp and Tyr residues showed a weak red shift, demonstrating the binding of triptolide to BSA was close to Trp and Tyr residues and that the hydrophobicity of the two residues decreased. When Δ□=15 nm, the slope was higher, showing that the fluorescence of BSA should be enormously attributed to Tyr residues and triptolide was closer to Tyr residues than Trp residues.

Binding mode and binding site between triptolide and BSA
Site marker competition experiments

There exist three similar domains (I, II, and III) in structure of BSA, which are typically bound reversibly with ligands (Paul, et al., 2010; Teng et al., 2011). The ligands can simultaneously bind to BSA by competitive binding and non-competitive binding mechanism. To recognize the binding region of triptolide upon BSA, the site probes ibuprofen and phenylbutazone, which are specifically bound to the known region or site on BSA (Sreerama and Woody, 1993; Bian, et al., 2006), are chosen for the site marker competition experiments.

The data were analyzed employing the Equation 3. The results were displayed in Figure 2D and Table 3, respectively. Comparing with the presence of the ibuprofen, the log$K$ value of BSA with triptolide was remarkably higher in the absence of the ibuprofen site marker at 298 K, whereas phenylbutazone had a negligible effect about the binding process of triptolide to BSA. These results indicated the binding site of triptolide was situated in subdomain IIIA (site II) of BSA.

Molecular modeling

The docking program AutoDock 4.0 was used as simulating about the binding progress between triptolide and BSA. This program was used to systematically provide information about the precise binding sites on BSA, the exact conformation of triptolide at the binding sites, as well as the interaction between triptolide and BSA (Morris et al., 2009), which can confirm the previously obtained results.

Crystal structure of HSA (UniProtKB: P02768) can be downloaded at http://www.pdb.org/pdb/home/home.do, showed there exist two binding sites, with one for phenylbutazone in site I (subdomain IIA) and the other for ibuprofen in site II (subdomain IIIA) (Sardar et al., 2008; Carter and He,1990). A homology in amino acid sequence exists between BSA and HSA. Thus, in this study, the binding sites for triptolide tested have an equivalent to the known binding site for HSA. The best Autodock orientations for triptolide for the binding subdomain IIA and IIIA of BSA were investigated. The docking scores obtained are presented in Table 4. As showed in the table, Site II^2 had the lowest free energy of binding (ΔG^0). This result implied that Site II^2 was expected to be the best site for binding to BSA and was identical with what has been discussed in above study of the site marker competitive.

When it comes to the binding complex of BSA with triptolide, Site II^2 showed in the Figure 6 (A) was the regnant configuration with the lowest free energy of binding. And Figure 6 (B) shows triptolide combined with BSA via hydrogen binding, which was supported by six hydrogen bonds (Leu–504, Glu–377, Lys–374). Basing on the results that the sum of hydrogen bonding energy, Van der Waals energy, and desolvation free energy ($\Delta E2$) was more negative than electrostatic energy ($\Delta E3$) in Table 4, we can conclude that Van der Waals and hydrogen bonding interactions were the driving forces in the binding of triptolide with BSA. These results agree with those of thermodynamic parameter analysis.

Figure 6 (C) shows the amino acid around triptolide within 6 Å, including hydrophobic residues (Phe–229, Ala–233, Leu–234, Ala–236, Trp–237 Leu–350, Leu–354, Leu–370, Ala–373, Ala–378, Leu–504, Val–505), polar residues (Gly–351, Tyr–355, Glu–375, Tyr–376, Glu–377, Thr–501, Glu–502, Ser–503, Asn–506,) and charge residues (Arg–232 Asp–347, Arg–371, Lys–374). The binding site was located deeply in the hydrophobic cavities of subdomain IIIA and the binding, which would to settle at a more preferable position in BSA, had to traverse the amino acid residues on the surface in the vicinity of the binding site. The formation of hydrogen bonding might have benefited this progress. All these events promoted the conformation and stabilized the α-helix, which indicated that the addition of triptolide can increase the α-helical content of BSA. This result was exactly consistent with the result of CD measurement. Furthermore, Figure 6(D) shows the distances between triptolide and some fluorophores, which revealed that triptolide was closer to Tyr–376 than other fluorophores and was on difference with these conclusions of synchronous fluorescence spectroscopy.

Conclusions

The spectroscopic method and molecular modeling method were successively employed to study the interaction between triptolide and BSA activity. These data revealed that static quenching was the mechanism of the quenching of the fluorescence of BSA by triptolide. It can be concluded that triptolide can spontaneously bind with BSA according to the experiment of binding capacity and calculated thermodynamic parameters. Both site-competitive replacement experiment and docking study indicated that subdomain IIA was the certain site that triptolide bound with BSA. Via the method of docking, the precise binding site was also probed. We also drew a conclusion that the microenvironment and conformation of BSA changed when triptolide was added by CD spectra and synchronous fluorescence. Van der Waals force and hydrogen bond were proven to have significant functions in the

binding process. The results obtained in this study provided important insights into the interaction mechanism between BSA and triptolide. Hence, this study could serve as a reference for pharmacological and clinical research on triptolide.

Acknowledgements

We gratefully acknowledge financial support from Hansoh Youth Talents Science Fund Project (No. QN150304). We also thank Dr. Chunying Gao, Dr. Jiangbo Du and Miss Yi Xu for editing the manuscript for English Language.

References

1. Bian, H.D., Li, M., Yu, Q., Chen, Z.F., Tian, J.N., Liang H. (2006). Study of the interaction of artemisinin with bovine serum albumin. Int. J. Biol. Macromol., 39: 291-297.
2. Cameron M., Gagnier, J.J., Little, C.V., Parsons, T.J., Blümle, A., Chrubasik, S. (2009). Evidence of effectiveness of herbal medicinal products in the treatment of arthritis. Part 2: Rheumatoid arthritis. Phytother. Res., 23: 1647–1662.
3. Carter, D.C., Ho, J.X. (1994). Structure of serum albumin, Adv. Protein Chem., 45: 153–176.
4. Carter, D.C., He, X.M. (1990). Structure of human serum albumin. Science., 249: 302–303.
5. Diao X.X., Deng P., Xie C., Li X.L., Zhong D.F., Zhang Y.F., Chen X.Y. (2013) Metabolism and pharmacokinetics of 3-n-butylphthalide (NBP) in humans: the role of cytochrome P450s and alcohol dehydrogenase in biotransformation. Drug. Metab. Dispos., 41:430-444
6. Diao X.X., Zhong K., Li X.L., Zhong D.F., Chen X.Y.(2015) Isomer-selective distribution of 3-n butylphthalide (NBP) hydroxylated metabolites, 3-hydroxy-NBP and 10-hydroxy-NBP, across the rat blood-brain barrier. Acta. Pharmacol. Sin., 36:1520-1527.
7. Greenfield, N.J., Fasman, G.D. (1969). Computed circular dichroism spectra for the evaluation of protein conformation. Biochem., 8: 4108–4116.
8. Hu, Y.J., Liu, Y., Zhang, L.X., Zhao, R.M., Qu, S.S. (2005). Studies of interaction between colchicine and bovine serum albumin by fluorescence quenching method. J. Mol. Struct., 750: 174–178.
9. Klajnert, B., Bryszewska, M. (2002). Fluorescence studies on PAMAM dendrimers interactions with bovine serum albumin. Bioelectrochem., 55: 33–35.
10. Liu, J., Wu, Q.L., Feng, Y.H., Wang, Y.F., Li, X.Y., Zuo, J.P. (2005). Triptolide suppresses CD80 and CD86 expressions and IL–12 production in THP–1 cells. Acta. Pharmacol. Sin., 26: 223–227.
11. Lou, Y.J., Jie, J., Wang, Y.G. (2005). Triptolide inhibits transcription factor NF–kappaB and induces apoptosis of multiple myeloma cells. Leuk. Res., 29: 99–105.
12. Liu, L., Jiang, Z., Liu, J., Huang, X., Wang, T., Zhang, Y., Zhou, Z., Guo, J., Yang, L., Chen, Y., Zhang, L. (2010). Sex differences in subacute toxicity and hepatic microsomal metabolism of triptolide in rats. Toxicology., 271: 57–63.
13. Lakowicz, J.R. (2009). Principles of fluorescence spectroscopy. Springer,.
14. Lakowicz, J.R., Weber, G. (1973). Quenching of fluorescence by oxygen. A probe for structural fluctuations in macromolecules. Biochem,. 12: 4161–4170.
15. Lu, J.Q., Jin, F., Sun, T.Q., Zhou, X.W. (2007). Multi–spectroscopic study on interaction of bovine serum albumin with lomefloxacin–copper(II) complex. Int. J. Biol. Macromol., 40: 299–304.
16. MacManus–Spencer, L.A., Tse, M.L., Hebert, P.C., Bischel, H.N., Luthy, R.G. (2010). Binding of perfluorocarboxylates to serum albumin: a comparison of analytical methods, Anal. Chem., 82: 974–981.
17. Mallick, A., Haldar, B., Chattopadhyay, N. (2005). Spectroscopic investigation on the interaction of ICT probe 3-acetyl-4-oxo-6,7-dihydro-12H Indolo-[2,3-a] quinolizine with serum albumins. J. Phys. Chem. B., 109: 14683-14690.
18. Matlin, S.A., Belenguer, A., Stacey, V.E., Qian, S.Z., Xu, Y., Zhang, J.W., Sanders, J.K., Amor, S.R., Pearce, C.M. (1993). Male antifertility compounds from Tripterygium wilfordii Hook f. Contraception., 47: 387–400.
19. Mei, Z., Li, X., Wu, Q., Hu, S., Yang, X. (2005). The research on the anti–inflammatory activity and hepatotoxicity of triptolide–loaded solid lipid nanoparticle. Pharmacol. Res., 51: 345–351.
20. Morris, G.M., Huey, R., Lindstrom, W. (2009). AutoDock4 and AutoDockTools4: Automated docking with selective receptor flexibility. J. Comput. Chem., 30: 2785–2791.
21. Ni, B., Jiang, Z., Huang, X., Xu, F., Zhang, R., Zhang, Z., Tian, Y., Wang, T., Zhu, T., Liu, J., Zhang, L. (2008). Male reproductive toxicity and toxicokinetics of triptolide in rats. Arzneimittelforschung., 58: 673–680.
22. Olson, R.E., Christ, D.D. (1996). Plasma protein binding of drugs, Annu. Rep. Med. Hem., 1: 327–337.
23. Panichakul, T., Wanun, T., Reutrakul, V., Sirisinha, S. (2002). Synergistic cytotoxicity and apoptosis induced in human cholangiocarcinoma cell lines by a combined treatmentwith tumor necrosis factor–alpha (TNF–alpha) and triptolide. Asian. Pac. J. Allergy. Immunol., 20: 167–173.
24. Paul, B.K., Samanta, A., Guchhait, N. (2010). Exploring hydrophobic subdomain IIA of the protein bovine serum albumin in the native, intermediate, unfolded, and refolded states by a small fluorescence molecular reporter, J. Phys. Chem. B., 114 6183–6196.
25. Ross, P.D., Subramanian, S. (1981). Thermodynamics of protein association reactions: forces contributing to stability, Biochem., 20: 3096–3102.
26. Sardar, P.S., Samanta, S., Maity, S.S., Dasgupta, S., Ghosh, S. (2008). Energy transfer photophysics from serum albumins to sequestered 3–hydroxy–2–naphthoic acid, an excited state intramolecular proton–transfer probe. J. Phys. Chem. B., 112: 3451–3461.
27. Sklar, L.A., Hudson, B.S., Simoni, R.D. (1977). Conjugate polyene fatty acids as fluorescent membrane probes: binding to bovine serum albumin. Biochem., 16, 5100–5108.

28. Shi, J.H., Wang, J., Zhu Y.Y., Chen, J. (2014). Characterization of intermolecular interaction between cyanidin-3-glucoside and bovine serum albumin: spectroscopic and molecular docking methods. Luminescence., 29: 522-530.
29. Sreerama, N., Woody, R.W. (1993). A self–consistent method for the analysis of protein secondary structure from circular dichroism. Anal. Biochem., 209: 32–44.
30. Tian, J., Liu, J., Zhang, J., Hu, Z., Chen, X. (2003). Fluorescence studies on the interactions of barbaloin with bovine serum albumin. Chem. Pharm. Bull., 51: 579–582.
31. Teng, Y., Liu, R.T., Li, C., Zhang, P.J. (2011). The interaction between 4-aminoantipyrine and bovine serum albumin: multiple spectroscopic and molecular docking investigations. J. Hazard. Mater. 190: 574-581.
32. Veatch W, Stryer L. (1977). The dimeric nature of the gramicidin A transmembrane channel: conductance and fluorescence energy transfer studies of hybrid channels. J. Mol. Biol., 113: 89–102.
33. Wang,YP, Wei, Y.L., Dong, C. (2006). Study on the interaction of 3,3–bis(4–hydroxy–1–naphthyl)–phthalide with bovine serum albumin by fluorescence spectroscopy. J. Photochem. Photobiol. A., 177: 6–11.
34. Wang, N., Ye, L., Yan, F., Xu, R. (2008). Spectroscopic studies on the interaction of Azelnidipine with bovine serum albumin. Int. J. Pharm., 351: 55–60.
35. Ware, W.R. (1962). Oxygen quenching of fluorescence in solution: an experimental study of the diffusion process. J. Phy. Chem., 66: 455–458.
36. Wang, C., Wu, Q.H., Wang, Z., Zhao, J. (2006). Study of the interaction of carbamazepine with bovine serum albumin by fluorescence quenching method. Anal. Sci., 22: 435–438.
37. Wang, Y.Q., Chen, T.T., Zhang, H.M. (2010). Investigation of the interaction of lysozyme and trypsin with biphenol A using spectroscopic methods.Spectrochim. Acta Part A Mol. Biomol. Spectrosc., 75: 1130–1137.
38. Yang, S., Chen, J., Guo, Z., Xu, X.M., Wang, L., Pei, X.F., Yang, J., Underhill, C.B., Zhang, L. (2003). Triptolide inhibits the growth and metastasis of solid tumors. Mol. Cancer. Ther., 2: 65–72.
39. Zhang, Y.Z., Zhou, B., Zhang, X.P., Huang, P., Li, C.H., Liu, Y. (2009). Interaction of malachite green with bovine serum albumin: determination of the binding mechanism and binding site by spectroscopic methods, J. Hazard. Mater., 163: 1345–1352.